COMMUNICATION

ChemComm
www.rsc.org/chemcomm

Transient FTIR spectroelectrochemical and stopped-flow detection of a mixed valence {Fe(I)–Fe(II)} bridging carbonyl intermediate with structural elements and spectroscopic characteristics of the di-iron sub-site of all-iron hydrogenase

Mathieu Razavet,[a] Stacey J. Borg,[b] Simon J. George,[a] Stephen P. Best,*[b] Shirley A. Fairhurst[a] and Christopher J. Pickett*[a]

[a] *Department of Biological Chemistry, John Innes Centre, Norwich, UK NR4 7UH. E-mail: chris.pickett@bbsrc.ac.uk*

[b] *School of Chemistry, University of Melbourne, 3010 Victoria, Australia*

Received (in Cambridge, UK) 20th December 2001, Accepted 6th February 2002
First published as an Advance Article on the web 5th March 2002

Iron(I) in biology?: one-electron oxidation of an {Fe(I)–Fe(I)} carbonyl cyanide precursor bearing a proximal thioether group leads to an {Fe(I)–Fe(II)} bridging carbonyl transient with spectral features similar to the di-iron sub-site of the CO inhibited paramagnetic centre of all-iron hydrogenase.

X-Ray crystallographic data for Fe-only hydrogenases isolated from *Desulfovibrio desulfuricans*[1] and *Clostridium pasteurianum*[2] together with infra-red evidence show that the active centre of the enzyme possesses a {2Fe3S} sub-site at which CO and CN ligands are bound.[3] The two Fe-atoms of the sub-site share two bridging sulfur ligands of a 1,3-propanedithiolate or related azadithiolate unit[4] with one of the Fe atoms additionally sulfur-ligated by a cysteinyl ligand bridged to a {4Fe4S}-cluster. This cluster/sub-site assembly is termed the H-cluster, Scheme 1.

The sub-site is paramagnetic (S = 1/2) in the oxidised, catalytically active form of the H-cluster (H_{ox}) and also in the CO inhibited form of this state, {H_{ox}(CO)}.[5–9] There is much current discussion as to whether these mixed valence states formally involve {Fe(III)–Fe(II)} or {Fe(I)–Fe(II)}-centres.[5a,6,9] The latter implies an unprecedented role for Fe(I) sites.

Herein we report spectroelectrochemical and stopped-flow FTIR studies of synthetic di-iron systems which address this oxidation-state issue.

The complexes $[Fe_2(S_2C_3H_6)(CN)_2(CO)_4]^{2-}$ **A**[10] and $[Fe_2\{MeSCH_2C(Me)(CH_2S)_2\}(CN)_2(CO)_4]^{2-}$ **B**[11] are unambiguously Fe(I)–Fe(I) species, Scheme 1, and thus appropriate candidates for the generation of higher oxidation state di-iron species relevant to the sub-site. Preparative scale oxidation of **B** leads to an unresolved mixture of carbonyl species whilst for **A** it leads to general decomposition involving extensive loss of CO band intensity. We therefore turned to transient methods in order to obtain information on primary oxidative processes of these species.

Cyclic voltammetry shows that both complexes oxidise irreversibly at 23 °C in MeCN or CH_2Cl_2–0.2 M $[NBu_4][BF_4]$ at vitreous carbon with E_p (**A**) = −0.11 V and E_p (**B**) = −0.25 V *versus* SCE (100 mV s^{-1}, MeCN electrolyte) in a one-electron step. Whereas the oxidation of **B** leads to the formation of a species **C** which undergoes a second, partially reversible, oxidation at −0.11 V *versus* SCE, which is fully reversible and overlaps the primary irreversible process at −40 °C, **A** only displays irreversible chemistry, even at −40 °C. Holding the potential at −0.25 V *versus* SCE prior to scan-reversal allows the build-up of a product which undergoes partially reversible reduction at −0.71 V *versus* SCE and leads to the re-generation of **A** (see below).

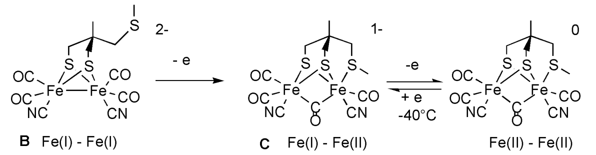

Scheme 1

Examination of the oxidation of **B** by thin-layer FTIR reflectance spectroelectrochemistry[12] under conditions concordant with the voltammetry (5 s oxidation step, MeCN electrolyte, vitreous carbon) showed well-defined differential absorption spectra as shown in Fig. 1(a). Thus oxidation at a potential which encompasses the primary process at −0.25 V *versus* SCE† led to the concerted growth of the higher frequency bands of **C** at 1978 and 2030 cm^{-1} and a *bridging* CO band at 1790 cm^{-1}. The appearance of the bridging CO band shows that structural rearrangement accompanies the irreversible electron-transfer. Re-reduction at a potential encompassing the reduction at −0.71 V *versus* SCE leads to the regeneration of *ca.* 80% of the starting material **B**. This indicates substantial conservation of the {2Fe3S} assembly in the oxidation/reduction cycle. Oxidation of **B** in (non-coordinating) CH_2Cl_2 gave an essentially identical spectrum to that of **C** obtained in MeCN showing that the latter is not involved in the oxidation process (*cf.* cyclic voltammetry).

Chemical oxidation of **B** was also studied by stopped-flow FTIR spectroscopy[13] in MeCN using one equivalent of ferrocinium ion as an oxidant ($E^{o\prime}$ = 0.38 V *versus* SCE,

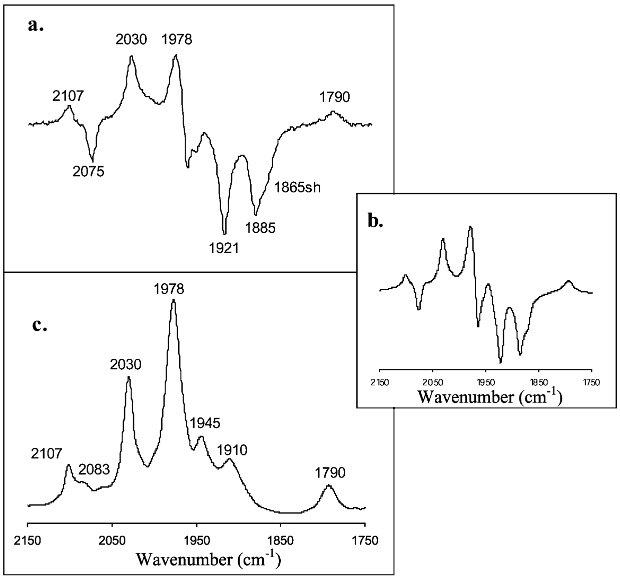

Fig. 1 (a) Differential absorbtion spectrum for electrochemical oxidation of **A** in an MeCN electrolyte at vitreous carbon under CO; (b) corresponding spectrum following one-electron chemical oxidation of **A** by ferrocinium cation obtained by stopped-flow FTIR spectroscopy; (c) absorbtion spectrum obtained 5 s after mixing in a stopped-flow experiment under CO.

DOI: 10.1039/b111613b

MeCN–0.2M $[NBu_4][BF_4]$). The differential absorption spectrum is essentially identical to that observed by thin-layer FTIR spectroelectrochemistry, Fig. 1(b). Varying the ratio of the reactants established the stoichiometry of the oxidation of **B** as a one-electron process as observed by cyclic voltammetry (Scheme 1). Spectra recorded under CO were cleaner and more intense than under N_2, indicating that (reversible) loss of CO was a decomposition pathway for **C**. The sensitivity of stopped-flow FTIR instrumentation allowed direct observation of the absorption spectra and revealed growth bands masked in the differential spectra by the depletion features (negative bands) of **B**. Under carbon monoxide two absorptions at 1945 and 1910 cm^{-1} are evident, Fig. 1(c). Under dinitrogen the band at 1910 cm^{-1} is relatively more intense and a shoulder is observed at 1900 cm^{-1} together with weak higher energy features indicative of chemistry involving CO loss.

The ν(CO) and ν(CN) bands of the parent dianions **A** and **B** are superimposable because the primary coordination spheres of the Fe atoms are essentially identical. Spectroelectrochemical and stopped-flow studies of the oxidation of **A** under identical conditions to those employed for **B** led to a depletion of the parent bands of **A**, but only weak growth bands are observed with no evidence for the formation of a bridging CO intermediate. The difference in the primary oxidation chemistry must clearly rest with **B** possessing a pendant thioether ligand, which is poised to attack the proximal iron centre, Scheme 1. That such a pendant thioether is capable of ligating an Fe atom in this fashion has been crystallographically established for neutral $[Fe_2\{MeSCH_2C(Me)(CH_2S)_2\}(CO)_5]$,[11] for the mono-anion $[Fe_2\{MeSCH_2C(Me)(CH_2S)_2\}(CN)(CO)_4]^-$ **D**,[14] and spectroscopically for the thermally unstable di-anion $[Fe_2(\mu\text{-}CO)\{MeSCH_2C(Me)(CH_2S)_2\}(CN)_2(CO)_3]^{2-}$ **E**.[11,14] That such an intramolecular nucleophilic attack can lead to a bridging CO group has been revealed by recent detailed stopped-flow FTIR kinetic and isotopic labelling studies of the conversion of **D** to **E**: nucleophilic attack by cyanide on the SMe ligated (less electron-rich) iron atom of **D** shifts a terminal CO group into the bridging mode to produce **E**.[14]

Implicit in one-electron oxidation of **B** to **C** is that the latter is paramagnetic. A solution of **B** in MeCN was oxidised with one equivalent of ferrocinium dissolved in the same solvent and the solution was frozen in isopentane (−140 °C) 11 s after mixing. Fig. 2 shows the well-defined $S = 1/2$ rhombic EPR signal obtained for the sample at 10 K. The values of the g-factor are 2.017, 2.006, and 1.988 which compare with 2.032, 2.017, and 1.998 for $\{H_{ox}\ (CO)\}$ of hydrogenase II from *Clostridium pasteurianum* reported by Adams.[15]

Table 1 shows a comparison of the spectral data for **C** with the FTIR and assignments for $\{H_{ox}(CO)\}$ for the *Desulfovibrio desulfuricans* all-iron hydrogenase given by De Lacey *et al.*,[9] together with FTIR data for **B**, **D** and **E**. There is clearly a close correspondence of FTIR frequencies for **C** with those of $\{H_{ox}(CO)\}$. Taken together with the observation of an $S = 1/2$ EPR signal, the data strongly support the sub-site of $\{H_{ox}(CO)\}$ being an {Fe(I)–Fe(II)} mixed valence assembly.

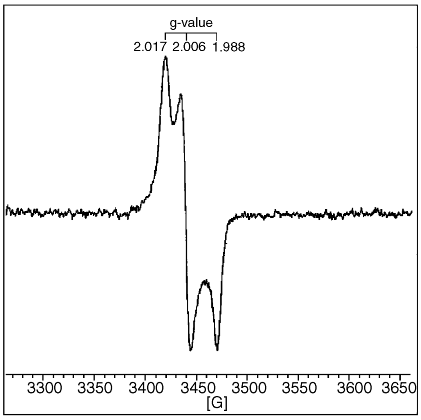

Fig. 2 EPR spectrum obtained in MeCN glass at 10 K after oxidation of **A** with ferrocinium cation and freezing at +133 K 11 s after mixing at room temperature. Recorded at 1 mW power and 0.1 mT modulation amplitude.

Table 1 Comparative FTIR data (cm^{-1})

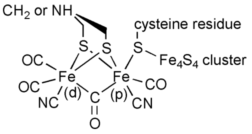		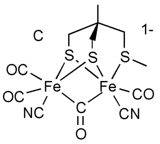	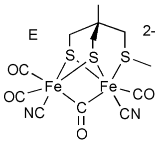
$\{H_{ox}(CO)\}$[12]		Fe(I)–Fe(II)	Fe(I)–Fe(I)
Bridging CO	1811	1790	1780
(p) Proximal CO	1965	1945 (1910)	1878
(d) Distal CO	1972	1978	1919
	2016	2030	1957
Distal CN	2089	2083	2075
Proximal CN	2096	2107	2083

In summary, we have shown that a transient bridging CO intermediate can be generated by one-electron oxidation of an {Fe(I)–Fe(I)} precursor bearing a proximal thioether group and that the observed CN, $CO_{terminal}$ and $CO_{bridged}$ infra-red stretching frequencies of this intermediate are consistent with the di-iron sub-site of $\{H_{ox}(CO)\}$ possessing an {Fe(I)–Fe(II)} unit.

We thank the ARC, BBSRC and the John Innes Foundation for supporting this work.

Notes and references

† Applied potentials in the spectroelectrochemical experiments were chosen to compensate for the intrinsic high resistivity of the thin-layer cell geometry.

1 Y. Nicolet, C. Piras, P. Legrand, C. E. Hatchikian and J. C. Fontecilla-Camps, *Structure*, 1999, **7**, 13.
2 J. W. Peters, W. N. Lanzilotta, B. J. Lemon and L. C. Seefeldt, *Science*, 1998, **282**, 1853.
3 A. J. Pierik, M. Hulstein, W. R. Hagen and S. P. J. Albracht, *Eur. J. Biochem.*, 1998, **258**, 572.
4 Y. Nicolet, B. J. Lemon, J. C. Fontecilla-Camps and J. W. Peters, *TIBS*, 2000, **25**, 138.
5 (*a*) C. V. Popescu and E. Munck, *J. Am. Chem. Soc.*, 1999, **121**, 7877; (*b*) I. C. Zambrano, A. T. Kowal, L. E. Mortenson, M. W. W. Adams and M. K. Johnson, *J. Biol. Chem.*, 1989, **264**, 20 974; (*c*) G. Wang, M. J. Benecky, B. H. Huynh, J. F. Cline, M. W. W. Adams, L. E. Mortenson, B. M. Hoffman and E. Munck, *J. Biol. Chem.*, 1984, **259**, 14 328; (*d*) J. Tesler, M. J. Benecky, M. W. W. Adams, L. E. Mortenson and B. M. Hoffman, *J. Biol. Chem.*, 1986, **261**, 13 536.
6 A. S. Pereira, P. Tavares, I. Moura, J. J. G. Moura and B. H. Huynh, *J. Am. Chem. Soc.*, 2001, **123**, 2771.
7 B. J. Lemon and J. W. Peters, *Biochemistry*, 1999, **38**, 12 969.
8 Y. Nicolet, A. L. De Lacey, X. Vernede, V. M. Fernandez, E. C. Hatchikian and J. C. Fontecilla-Camps, *J. Am. Chem. Soc.*, 2001, **123**, 1596.
9 A. L. De Lacey, C. Stadler, C. Cavazza, E. C. Hatchikian and V. M. Fernandez, *J. Am. Chem. Soc.*, 2000, **122**, 11 232; Z. Cao and M. B. Hall, *J. Am. Chem. Soc.*, 2001, **123**, 3734.
10 E. J. Lyon, I. P. Georgakaki, J. H. Reibenspies and M. Y. Darensbourg, *Angew. Chem., Int. Ed.*, 1999, **38**, 3178; M. Schmidt, S. M. Contakes and T. B. Rauchfuss, *J. Am. Chem. Soc.*, 1999, **121**, 9736; A. Le Cloirec, S. P. Best, S. Borg, S. C. Davies, D. J. Evans, D. L. Hughes and C. J. Pickett, *Chem. Commun.*, 1999, 2285.
11 M. Razavet, S. C. Davies, D. L. Hughes and C. J. Pickett, *Chem. Commun.*, 2001, 847.
12 S. P. Best, S. A. Ciniawsky and D. G. Humphrey, *J. Chem. Soc., Dalton Trans.*, 1996, 2945.
13 S. J. George, G. A. Ashby, C. W. Wharton and R. N. F. Thorneley, *J. Am. Chem. Soc.*, 1997, **119**, 6450.
14 S. J. George, Z. Cui, M. Razavet and C. J. Pickett, unpublished.
15 M. W. W. Adams, *J. Biol. Chem.*, 1987, **262**, 15 054.